ASSESSMENT OF CLIMATE CHANGE IMPACTS ON WATER RESOURCES OF SEYHAN RIVER BASIN

Levent Tezcan[1], Mehmet Ekmekçi [1], Özlem Atilla[1], Dilek Gürkan[1], Orçun Yalçınkaya[1], Otgonbayar Namkhai[1], M. Evren Soylu[1], [2]Sevgi Donma, [2]Dilek Yılmazer, [2]Adil Akyatan, [2]Nurettin Pelen, [3]Fatih Topaloğlu, [4]Ahmet İrvem

[1]*International Research Center For Karst Water Resources-Hacettepe University (UKAM), Ankara*

[2]*DSI VI. District Adana*

[3]*University of Çukurova, Adana*

[4]*Mustafa Kemal University, Antakya*

1. Introduction

This research was conducted within the framework of a multi-disciplinary bi-lateral project supported by the Turkish Scientific and Technological Research Council (TUBİTAK) and the Research Institute for Humanity and Nature-Japan (RIHN). A total of 8 subgroups conducted their research independently but in coordination of the "Impact of Climate Change on Agricultural Production in Arid Areas" ICCAP. For several reasons, the Seyhan River Basin was selected as the pilot research area for the project. The water resources of the basin were studied by the International Research Center For Karst Water Resources (UKAM) of the Hacettepe University (Ankara) in cooperation with the DSI, University of Çukurova in Adana and Mustafa Kemal University in Antakya.

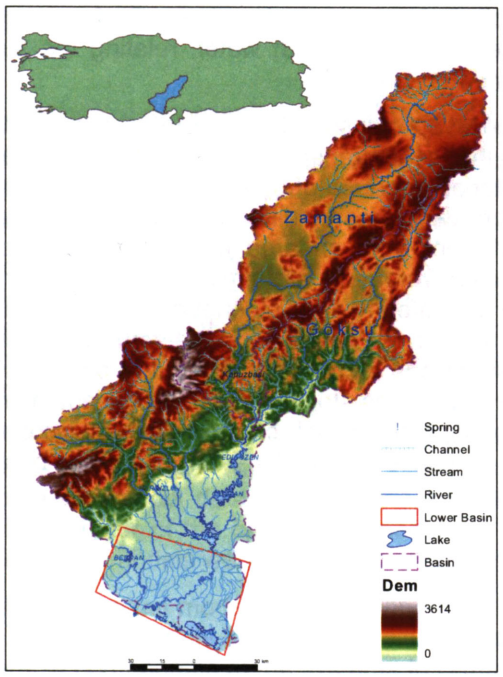

Figure 1.1 Geographical location and division of Seyhan River Basin according to type of water resources

The Seyhan River Basin, located at a semi-arid part of Turkey-having significant water and land resources potential- was selected as a pilot study area, to inspect the vulnerable components of water resources (surface water and groundwater) systems, and define and quantify their vulnerability to climate change. The Seyhan River Basin (SRB), one of the major water resources basins in Turkey is located in the Eastern Mediterranean geographical region of Turkey (Figure 1.1). The drainage area of the SRB is more than 21000 km^2 extending between 37°13'-40°12' N and 35°03' -37°56' E. Highland makes large parts of the basin, particularly in the northern areas. The basin is subdivided into two major parts with regard to water resources: the whole Seyhan River Basin (SRB) which was studied for the surface water resources of the basin and the Adana Plain (AP) that comprises the groundwater resources in the alluvial aquifer (see Figure 1.1).

2. Theoretical Conceptualization

Interactions between hydrological and biogeochemical systems, involves climatic conditions represented by meteorological parameters like precipitation and evapotranspiration, infiltration as the excess precipitation from interception and evaporation from surface storage, deep percolation to groundwater system and the factors controlling the biomass including nutrient uptake, decomposition and leaching and weathering. As depicted in Figure 2.1, the soil moisture seems to have not only the more linkages than other components, but also linkages with both surface and subsurface environment, implying that the soil zone plays a key role in the climate-soil-vegetation dynamics. This dynamics can be interrelated within a differential equation that describes the volumetric water change in the soil zone (Rodriguez-Iturbe, 2000).

$$nZ\frac{d\theta}{dt} = I(\theta,t) - E(\theta,t) - D(\theta,t) \tag{1}$$

where, n: porosity, Z: depth of soil zone, θ: soil moisture content, I(θ, t): infiltration into soil, E(θ, t): evapotranspiration, and D(θ, t): deep percolation to groundwater system.

The terms on the right hand side of Equation 1, are all functions of θ, the soil moisture content. Infiltration depends on the saturation degree of the soil. In other words, infiltration does not exceed the available void volume in the soil during a particular storm. Surface runoff is assumed to take place only when the substrate is saturated with water, relating the surface runoff with the availability of water in the subcutaneous zone.

Vegetation and soil characteristics control the evapotranspiration to a large extent. Wilting point and field capacity are known to control the evapotranspiration. However, the rate of evapotranspiration depends on the type of vegetation because of different wilting point and the soil moisture allow maximum evapotranspiration vary among different types of vegetation. Evapotranspiration in forested area is quite different from an area covered by herbaceous vegetation even when climatic conditions and soil environments are similar. The last term, deep percolation is apparently under the control of the saturated hydraulic conductivity, soil water and soil characteristics. This relation is generally given as Ks θ_c , where Ks is the saturated hydraulic conductivity, θ is the soil moisture and the exponent c is a constant dependent on the type of soil. Although the nature of equation (1) may be regarded as stochastic differential equation (e.g. Rodiguez-Iturbe, 2000) because of the fact the precipitation which controls the water content in the subcutaneous zone is a random process, it can be solved by for a certain basin by combining separate solutions for each term.

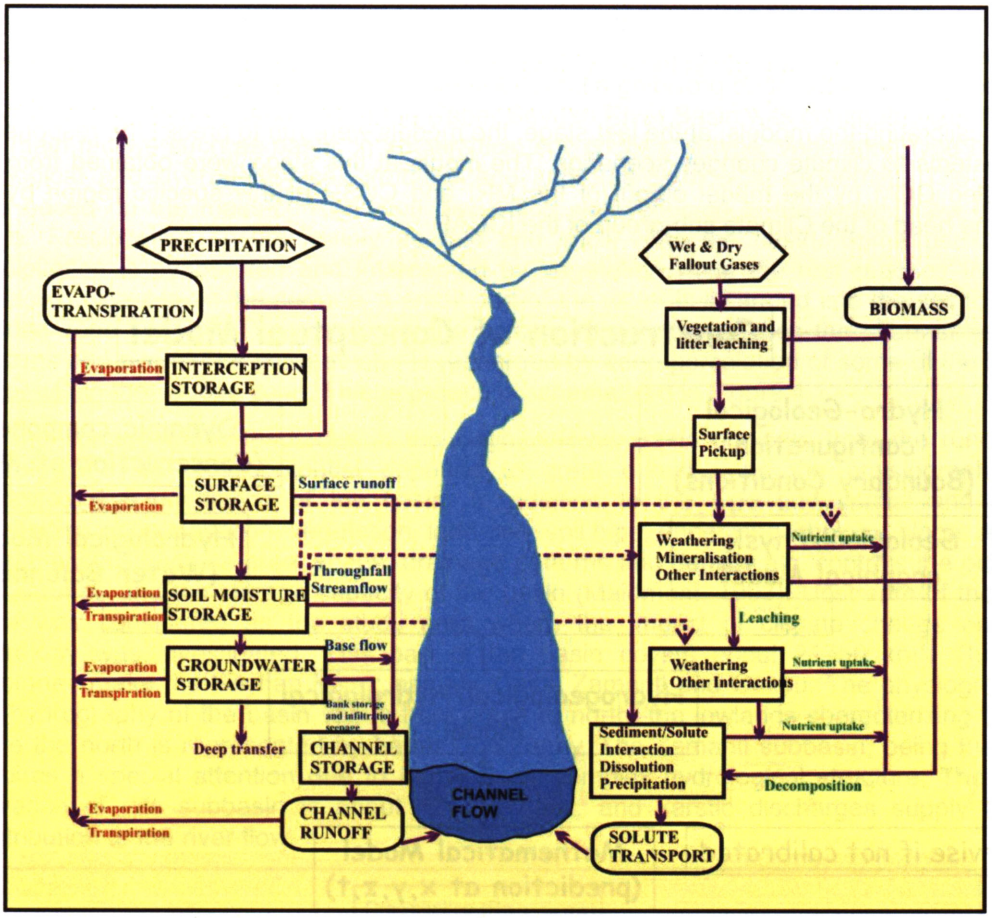

Figure 2.1. Simplified representation of the interaction of hydrological and biochemical processes operating in a drainage basin [from Webb and Walling, 1996: Rodriguez-Iturbe, 2000].

3. Technical Approach and Methodology

The approach followed in assessing the impacts of climate change on the water resources of the SRB is based on geographical information system (ArcGIS®) based modeling studies and comprises three major steps. The overall approach is schematized in Figure 3.1.

Following a comprehensive development of conceptual models, the water systems are simulated by numerically solved mathematical models. Although a holistic approach will be applied in defining the hydrological interactions between surface and subsurface water resources, the conceptual models were developed for interconnected surface and subsurface water systems separately.

The interactions then will be defined within the boundary conditions of each system. The conceptual models were developed based upon all geological, hydrogeological, hydrometeorological data including the spatial distribution of surface cover. The second step was the transfer of the conceptual models to appropriate mathematical models. The selected mathematical models were used for both informative and predictive purposes.

The conceptual models were defined on a grid by the initial and boundary conditions. They were calibrated to define the current situation of the systems and then will be run to specify the vulnerable components of the systems to climate changes. Regarding the aim of the project, the models will be run for vulnerability of parameters to climate changes. In this context, not only the input parameters, such as recharge regime but also the changes of boundary conditions as a consequence of climate change were reflected within the models. Therefore, the boundaries of the systems, particularly those of the groundwater system (aquifer) were set on site so as to

control the changes rather than estimating the groundwater potential to be managed. That is, the models were run for a purpose of the effects of climate changes on the behavior of the water resources systems rather than providing a base for a management strategy.

After calibrating the models, at the last stage, the models were run to predict the response of water systems to climate changes scenarios. The inputs at this stage were obtained from the downscaled GCM by the model output of the MRI and CCSR at this specific region by Dr. Kimura the head of the Climate sub-group of the ICCAP.

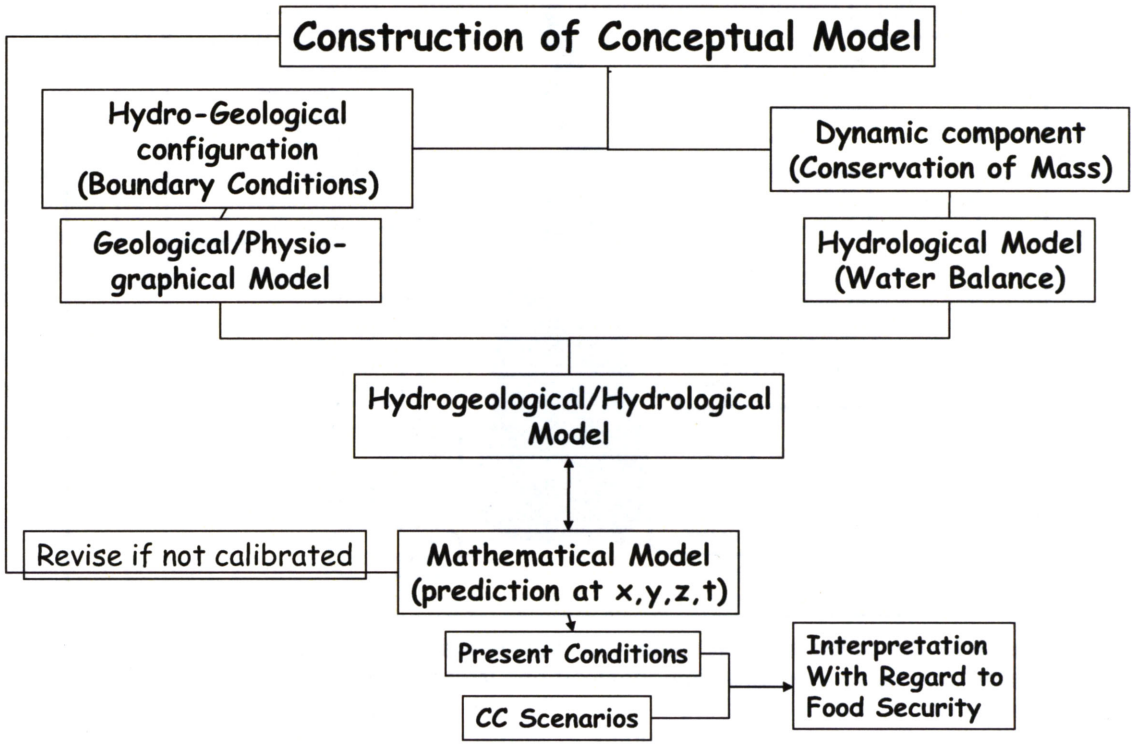

Figure 3.1. Schematic representation of the approach applied in the project studies

MIKE-SHE (Systeme Hydrologique Europeen), a software combining climate-soil-vegetation and groundwater systems was used to assess the interrelations between these systems in the Seyhan River Basin. The code has six modules for snowmelt, evapotranspiration, surface runoff, flow in the subcutaneous zone, channel flow and groundwater flow. The first two are calculated by analytical methods, while the surface runoff and channel flow are simulated by finite difference solution of the 2-D and 1-D Saint-Venant equation, respectively. The unsaturated flow is simulated by the finite difference solution of the 1-D Richards equation. Groundwater flow is simulated by the finite difference solution of the 3-D Boussinesq equation (Abbott et al, 2000). The MIKE-SHE software was used to simulate the surface hydrology of the mountainous Upper Seyhan Basin.

The Plain section, called the Adana Plain, is rather flat and has no significant surface flow. Therefore, another code that embodies the MODFLOW and MT3DMS in SEAWAT-2000 which also capable of simulating the variable density flow and solute transport, enabling simulation of sea water intrusion.

4. Characterization of the Water Resources Systems

Two major water resources systems exist in the Seyhan River Basin. The Seyhan Dam located at the northern edge of Adana city can be regarded as the approximate divide between the groundwater system and the surface water system. The groundwater system occurs in the alluvial plain extending from the Seyhan Dam site to the Mediterranean in the south (see Fig.

1.1).

4.1. Surface Water Resources in the Upper Seyhan River Basin

The surface water resources of the Upper Seyhan River Basin was conceptualized based on the main factors such as basin characteristics, soil cover and type, vegetation type and cover, geological and hydrogeological structure and hydrometeorological properties. The approach was based on the mass-conservation law which was reflected in the basin scale hydrologic cycle. Precipitation occurs mainly as rain and snow onto the basin. Some portion of the precipitation is evaporated and intercepted by vegetation while the rest reaches the ground surface. Once it is on the surface, a small part of the water is infiltrated into the soil to form the vadose zone storage. The rest forms the surface runoff that reaches the channel flow in the streams and rivers. The groundwater is recharged by deep percolation of some of the infiltrated water within the vadose zone. This approach is schematized in Figure 4.1.

The surface water resources in the Seyhan River Basin originate from the runoff of the hydrologic cycle. This potential depends to great extent upon the physiographical and meteorological conditions of the basin. In addition to the type and spatial and temporal distribution of precipitation, vegetation, land-use, soil type, underlying lithology, slope, and basin characteristics such as area, shape, drainage patterns and density etc. controls the occurrence of the runoff and the storage capacity of the basin (Maidment, 1993). Upstream of the Seyhan Dam was considered as the study area where the impact of climate change on surface hydrology was investigated. This part of the basin covers about 21750 km^2. Three main tributaries make the Seyhan River; namely, Cakit, Zamanti and Goksu. The physiography and oro-hydrography of the basin varies from south to north; the lowlands characterizing the south while the north is represented by harsh topography. The Zamanti subbasin, being the largest, requires a special attention due to its relatively complex hydrological structure. The average elevation of this subbasin is about 1250 m. asl., and karstic discharges supply the main contribution to the river flow.

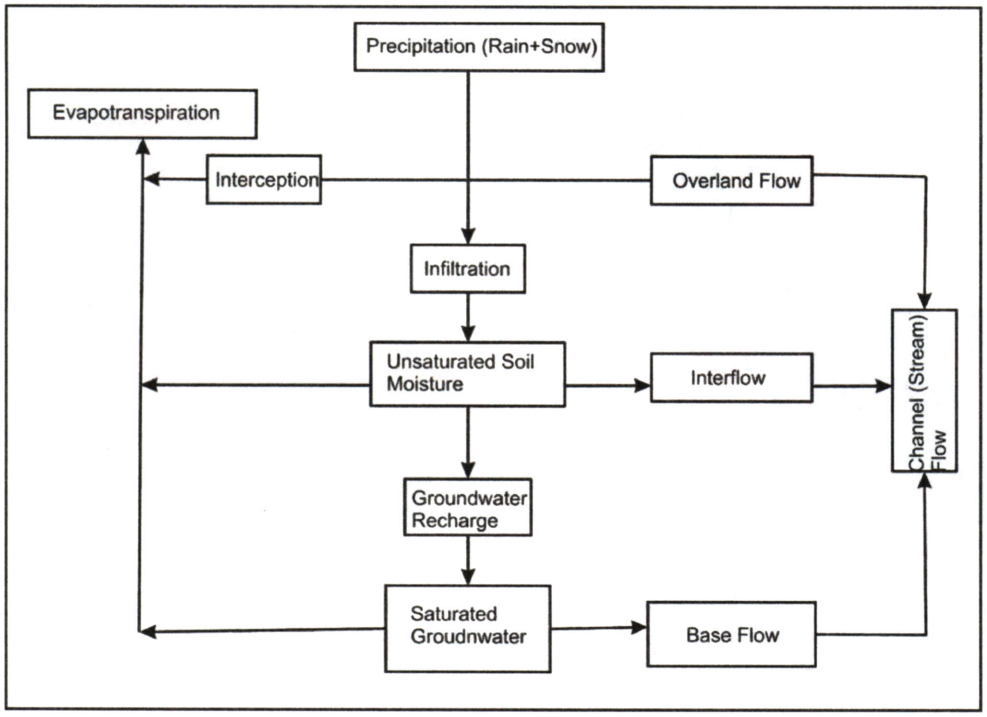

Figure 4.1. Schematic conceptualization of the surface hydrology system in the Upper Seyhan River Basin

Geologically the upper basin comprises lithological units representing a time span from Paleozoic to Quaternary (Figure 4.2). The Paleozoic is represented by carbonates and schists. Mesozoic units are made up of mainly carbonates and ophiolitic rocks while the extensive clastics, carbonates and evaporitic lithologies represent the Cenozoic units. Volcanic rocks are

of Neogene age. Alluvium, morain and slope wash are of Quaternary age. The pervious lithological units are generally made of carbonate rocks most of which are extensively karstified. The carbonate rocks that form karst aquifers constitute 6758.3 km^2 corresponding to about 30 % of the whole basin. The geological units arre classified into 8 units with respect to their relative permeabilities. In Figure 4.2, these 8 units are presented, where class 1 indicates the most permeable unit, and class 8 represents the less permeable unit.

In the higher elevations of the basin, the precipitation falls in the form of snow. In addition to its contribution to the runoff, the importance of the snowmelt stems from the fact that karst groundwater system contributes in significant amounts to the streamflow through numerous huge karstic springs. The karstic groundwater systems (aquifers) are recharged by the snowmelt as well as rainfall. Therefore, the change in type of precipitation should change the recharge conditions of karst aquifers which in turn will alter the stream flow regime of the Seyhan River.

4.2. Groundwater Resources in the Adana Plain

The Adana Plain geologically is composed of alluvium deposited mainly in deltaic and fluvial environments. Clearly, the tectonic development of the country is reflected in the deposition, because the thickness of the alluvium exceeds 1000 m. in some places. The surface area of the alluvial plain is 2211.9 km^2 corresponding to about 10 % of the total area of the basin. Owing to the heterogeneity that is evident from the boreholes, the groundwater reservoir is constituted by more than one aquifer separated by less permeable layers. On the other hand, because the lithological layer covering the upper aquifer is not homogenous, the aquifer is confined in some areas. That is the groundwater system is a multilayered system partly unconfined in the north and confined in the southern part. The general hydrogeological structure is depicted Figure 4.3.

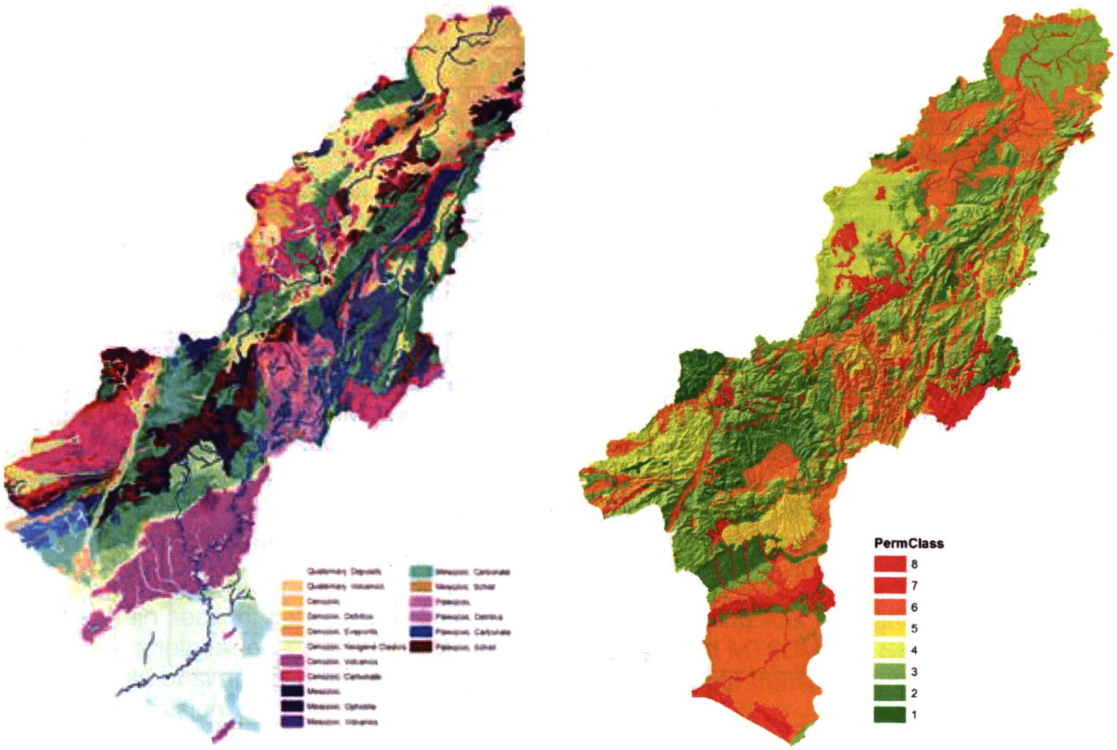

Figure 4.2. Simplified geological and permeability class maps of the Seyhan River Basin

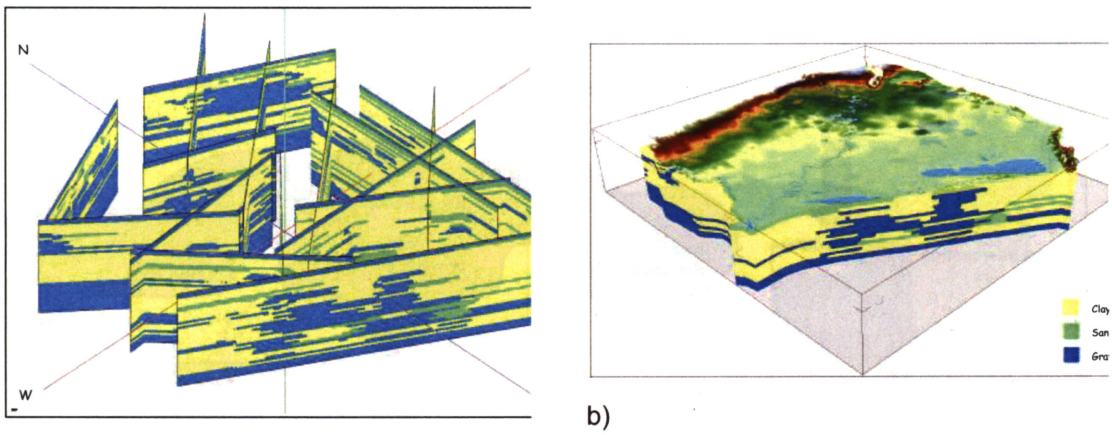

a) b)

Figure 4. 3. Simplified geological a) fence and b) block diagrams of the Adana Plain conceptualizing the hydrogeological structure

5. Modeling of the Water Resources in the Seyhan River Basin

5.1. Selected Mathematical Models

The surface hydrology of the Upper Seyhan River Basin was modeled by MIKE- Systeme Hydrologique Europeen (MIKE-SHE) a modular distributed parameter model combining all flow processes at the surface, in the vadose zone and the saturated zone. The model simulates the snow melt (analytical), evapotranspiration (analytical), flow in the vadose zone (1-D Richards equation), overland flow (2-D Saint-Venant equation), channel flow (1-D Saint Venant equation) and groundwater flow (3-D Boussinesq equation). The model uses the finite difference techniques in solving the partial differential equations. Structure of the modular model is depicted in Figure 5.1.

Following the hydrogeological characterization of the Adana alluvial plain, the conceptual model was transferred to the mathematical models. Sea water intrusion was also considered in the conceptual model. Therefore, in addition to the groundwater flow model, the seawater intrusion was also transferred to a mathematical model and run together with the groundwater flow model. MODFLOW (McDonald & Harbaugh, 1998) was used to simulate the groundwater flow while the sea water intrusion was simulated by SEAWAT-2000 (Langevin, et al., 2003), integrated with MODFLOW.

5.2. Preparation and Processing Relevant Data

5.2.1. Seyhan River Basin

The available data were designated, digitized and transferred to a geographical information system. The basin boundaries were defined according to the topographical divide. Topographical, geological and soil maps were digitized and input as separate layers. At the first phase the model was run to simulate the present conditions. Meteorological data estimated for the period between 1994-2003 by the RCM (Kimura, 2007) were used as input to the model in this simulation phase. All simulations were made on daily basis. The model was calibrated using the flow rates recorded at the gauging stations in the basin (Figure 5.2). The evapotranspiration was calculated by using the estimated parameters required for Penman-Monteith equation, and the root depth and the leaf area index (LAI). The LAI values are extracted from monthly MODIS satellite images for the period of 2000 - 2006. The MODIS images are obtained from the Boston University, Department of Geography, Climate and Vegetation research groups ftp site (ftp://primavera.bu.edu/pub/datasets). The monthly values for each year are averaged for each land class units given in Figure 5.3. The inter-annual change of the LAI is not taken into account. The monthly LAI distribution for each land units is given in Figure 5.4.

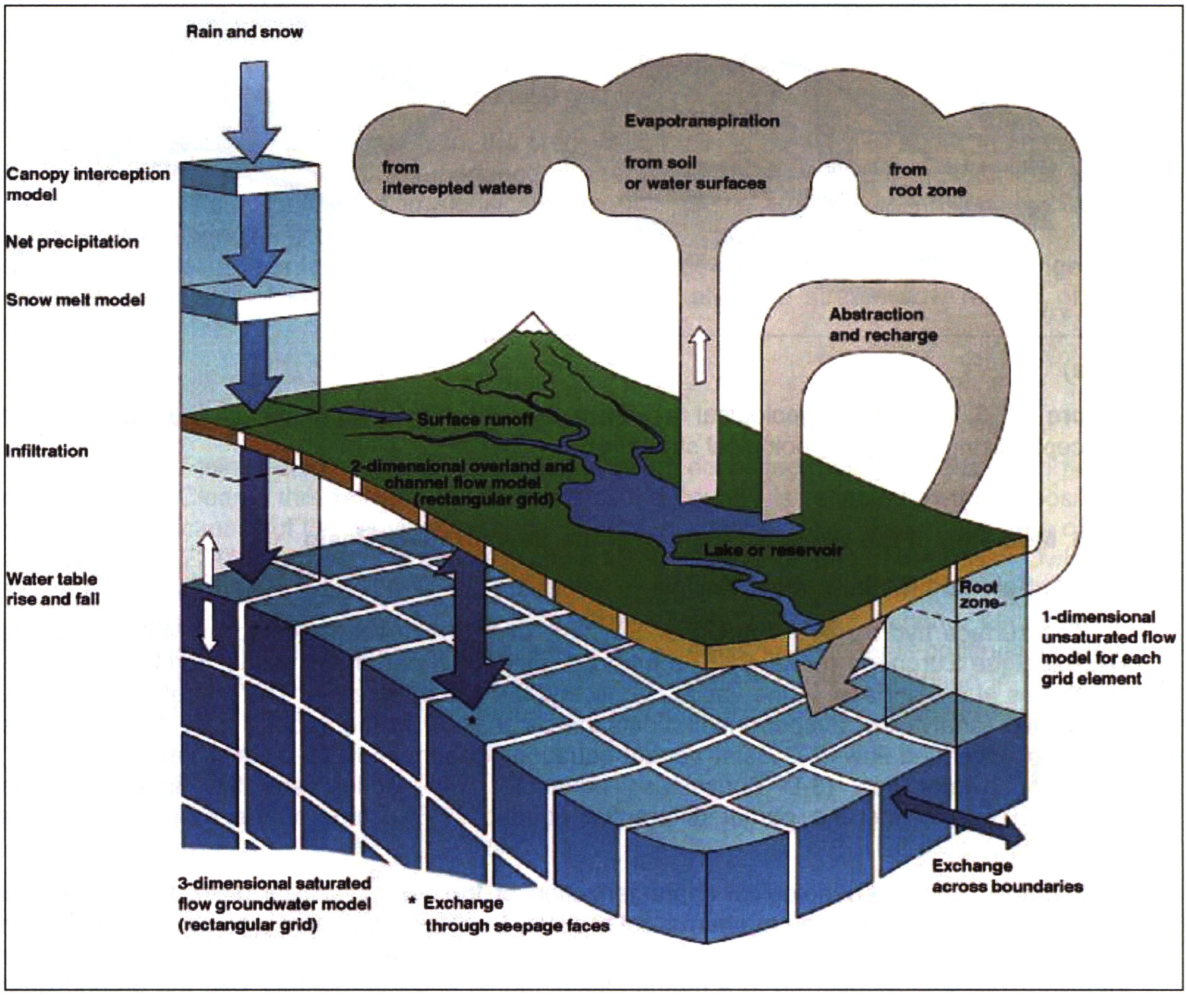

Figure 5.1. Modular structure of the MIKE-SHE model

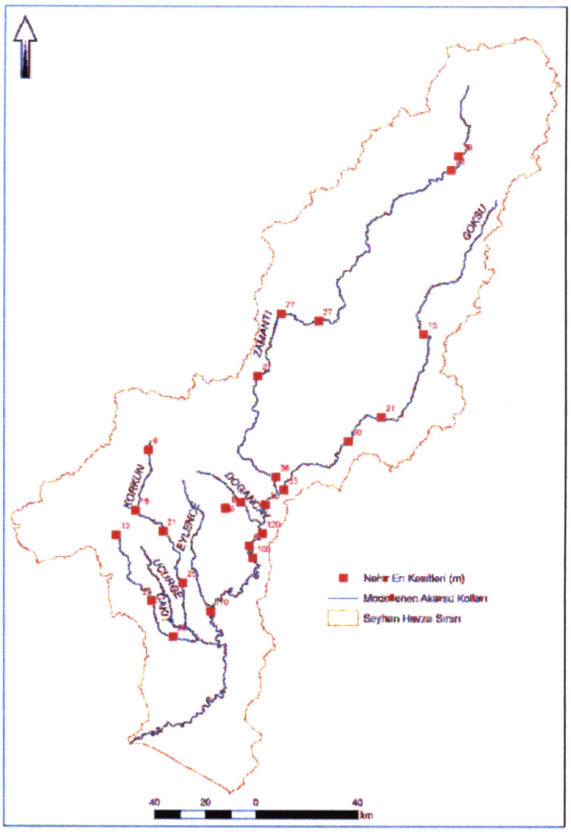

Figure 5.2. Sections where measurements were made for channel flow simulation

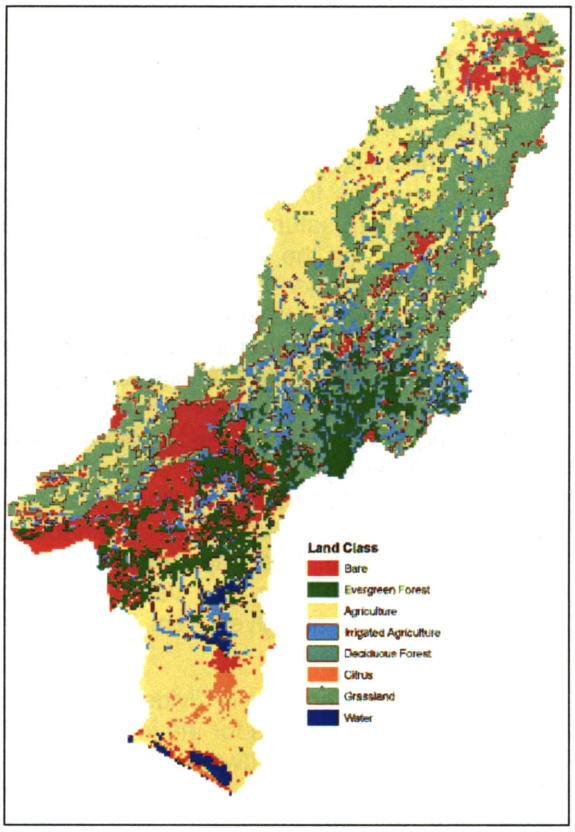

Figure 5.3. The land class units used for evaporation estimations

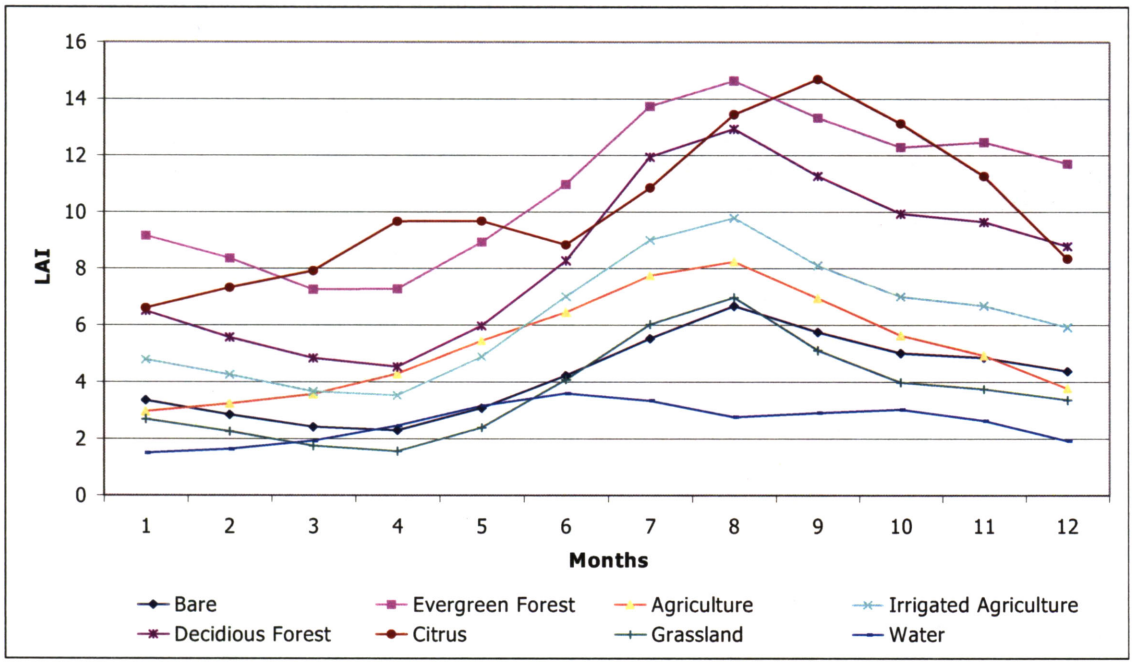

Figure 5.4. The monthly average LAI values depicted from MODIS images.

The basin was discretized into 216 x 299 finite difference grids of 1 km^2 each. The boundary of the basin was defined in the model by assigning the value indicating impervious unit in cells

that fall on the divide. The southern boundary of the basin is Mediterranean Sea, where the boundary is defined by fixed head and attributed with a head value of 0 for present conditions. For the warm-up conditions the fixed head value is taken as 80 cm.

Because the subsurface water is among the major factors that control evapo-transpiration rate and the infiltration, the vadose zone is taken into account in the model. The soil map was re-arranged so as to define the soil type and some model parameters like effective porosity, specific retention, saturated hydraulic conductivity, and Van Genuchten (1980) parameters that are used in solving the Richards equation were defined for two major types of soil in the basin. The vertical dimension of the vadose zone was taken as maximum 500 m. The depth to the groundwater level is taken as the lower boundary of the vadose zone, and the thickness of the vadose zone is calculated in each model time step according to the groundwater level. The vadose zone divided into 80 finite-difference layers of thickness varying between 0.1 to 10 m. The horizontal distribution of the vadose zone parameters are distributed to the basin by considering the shallow soil and underlying lithologic properties. The vertical zone is divided into three parameter layers. The upper zone is characterized by the soil thickness and structure; the lower layers are based on the lithological structures. A total of 37 distinct classes are defined and the vadose zone parameters are attributed for each class. The distribution of the classes is given in Figure 5.5. The saturated hydraulic conductivities for the vadose zone are within the range of 10^{-5} to 10^{-9} m/s. The Van Genuchten parameters for soil moisture – conductivity and retention relations are given from the literature values considering the average grain size for each class.

The groundwater zone is divided into two layers. In the upper layer, the impervious units are defined as confining units for the lower layer. The ophiolite, schist and clay units are defined as impermeable, and groundwater circulation is not allowed within these units (Figure 5.6). The thickness of the upper layer is taken as 200 m, where as it is taken as 1200 m for the lower layer.

The surface runoff was simulated by finite difference solution of the Saint Venant equation. Runoff occurs whenever the overland storage exceeds a certain threshold. Overland storage starts to develop when precipitation rate exceeds the infiltration capacity. The model parameters required in this calculation are the detention storage (Figure 5.7) and Manning number (Figure 5.8) which was distributed to the basin by considering the soil and land use classes.

Channel flow component was simulated using the geometry of the river bed defined by finite difference nodes. This required measurement of width and depth of the river at sections where flow rate was observed. The distance between river nodes ranges between 200 and 1500 m depending on the river morphology. More frequent nodes were defined where the river bends in shorter distances.

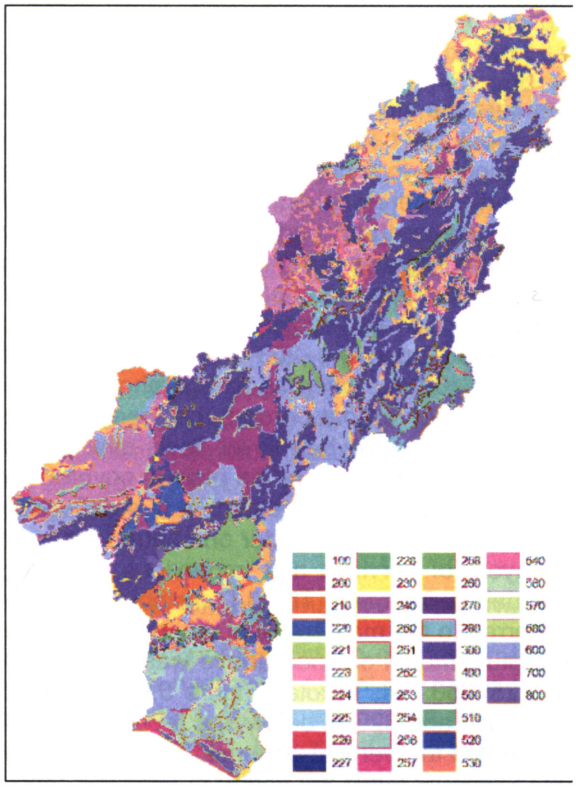

Figure 5.5. The classes of the vadose zone parameters

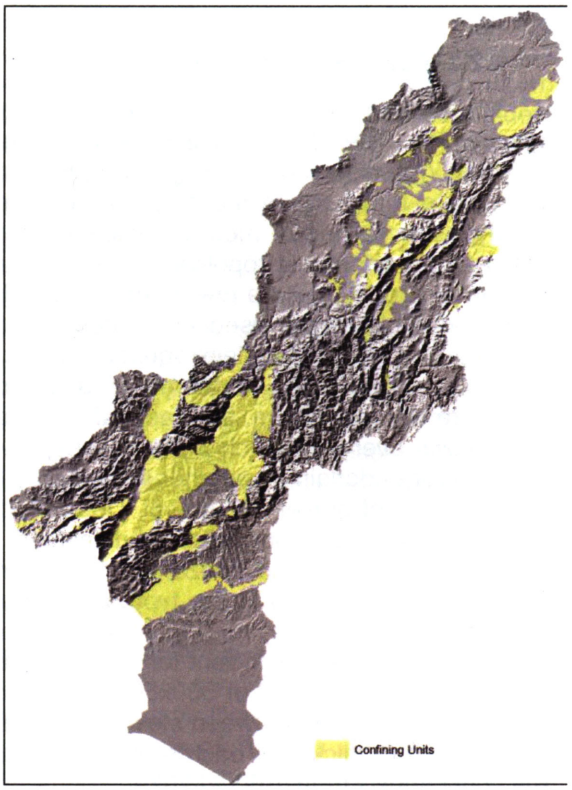

Figure 5.6. The distribution of the upper impervious confining units for groundwater circulation

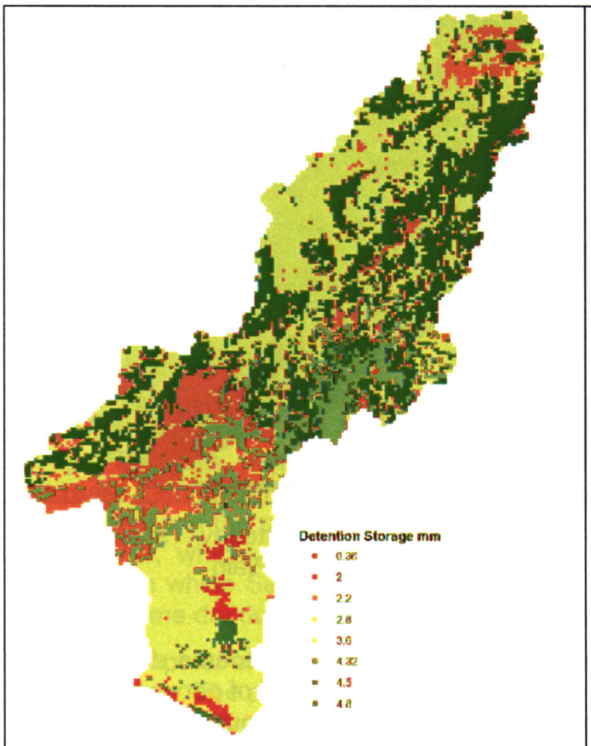

Figure 5.7. The spatial distribution of the detention storage values for overland flow

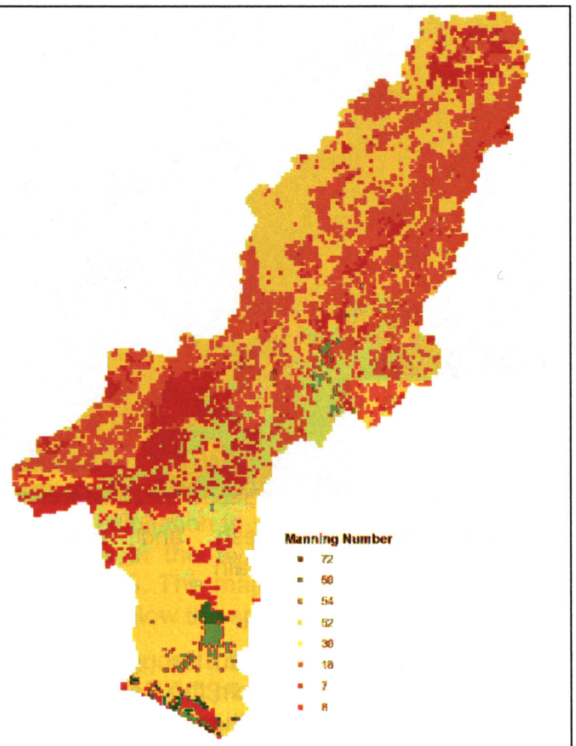

Figure 5.8. The spatial distribution of the Manning Numbers for overland flow

5.2.2. Adana Plain Aquifer

The Berdan-Tarsus river and Ceyhan River borders the study area from the west and east respectively. The plain aquifer covers an area of about 2271 km2, extending between these borders. Water demand for irrigation in the plain is supplied to a great extent from the Seyhan Dam Lake that borders the study area from the north. Therefore, only a certain number of boreholes were drilled, most of which are located in the northern part of the plain to supply water to the Adana Metropolitan city. However, after drip-irrigation system became attractive to the farmers in the plain, a few boreholes are drilled in the southern part of the plain. The data of these boreholes were used in conceptualizing the groundwater system. The geohydrologic characterization of the plain aquifer system was based upon the 203 well logs. Depth of boreholes drilled at the northern part does not exceed 100 m., whereas the boreholes at the south are deeper; 363 m. the deepest. The Tarsus-Berdan river that borders the area from the west, flows over a thick clay (impervious) layer. Similarly the Ceyhan River flows over a thin sandy layer underlain by another thick clayey layer. The northern part of the plain is covered by a succession of gravel-clay-gravel. Detailed study of the well logs suggests that it is difficult to distinguish more than one aquifer, but instead, it is more realistic to consider one heterogeneous aquifer with vertical and horizontal interfingering layers of pervious and impervious deposits; which is also supported by the type of the depositional environment. The 3-D distribution of the clay, sand and gravel layers (Figure 4.3) was transferred to the mathematical model assigning a distinctive hydraulic coefficient for each. The conceptual model outlined above was transferred to a finite difference grid of 500x500 m composing 250860 cells in total (Figure 5.9). The third dimension was taken between elevations of 20 m. above and 320 m below sea level. 20 model layers of 20 m thickness each were defined to represent the vertical dimension. The model is run continuously from 1993 to 2079.

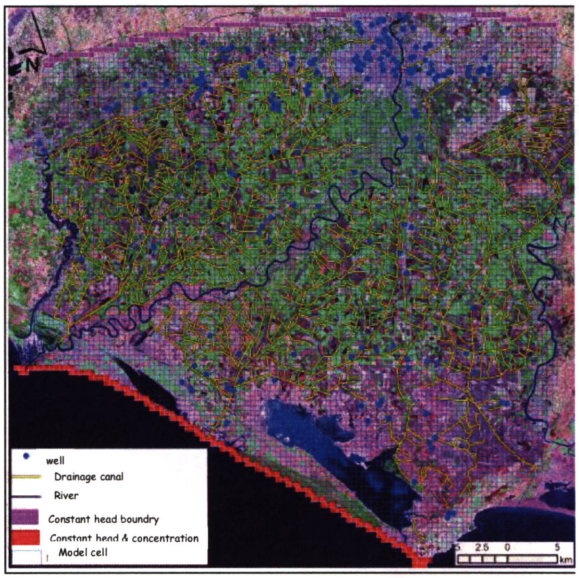

Figure 5.9. Grid mesh and boundary conditions in the Adana Plain

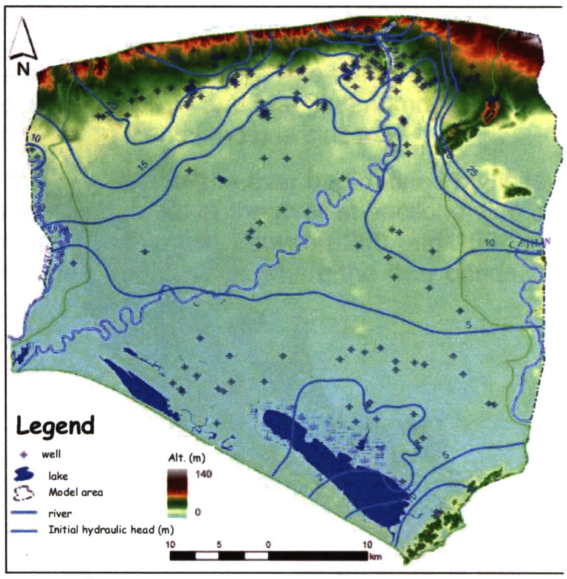

Figure 5.10. The steady state head distribution in the Adana Plain

The aquifer is recharged through direct rainfall onto the areas where coarse deposits are exposed, from seepage from the Seyhan River where the bed is composed of pervious material and through inflow the northern boundary. The recharge from the northern boundary is identified by stable isotope analysis in deep wells in the plain. The isotope content of the groundwater clearly indicates the recharge from higher elevations. Because the amount of the inflow through the northern boundary is difficult to predict and any prediction would associate significant uncertainty, the boundary condition was defined based upon the groundwater level

measurements in the boreholes close to this boundary. This provided that recharge through this boundary is computed by the model based on the gradient changes. The head values obtained by MIKE SHE simulation for present and warm-up conditions are given for the northern boundary for each time step. Discharge of the aquifer occurs as the outflow into the sea, effluent flow to the Seyhan River where hydrogeologic conditions are appropriate, and as groundwater abstraction through wells and drainage canals. The boundary condition at the south where the aquifer is in contact with the sea was taken as "constant head-concentration boundary" for the first 10 years; whereas this boundary was changed to "variable head-concentration boundary" during the second and third periods where the system is affected by the climate change. The concentration of the sea water was taken as 19200 mg/l of Cl from chemical analysis of the sea water. The initial head values were obtained by steady state simulations under natural conditions. The head is attributed as 0 for present conditions. Two different rates for the sea level increase are given to the model for warm up conditions. For the first 20 years, the sea level is assumed to reach to 40 cm, whereas it is assumed as 80 cm at the end of 2079. The groundwater utilization is also increased within these stress periods. The increase rate is taken as 20% for the first 20 years, and 50% for the rest. The locations of the new wells are attributed randomly.

6. Climate Change Impacts on the Water Resources of the Seyhan River Basin

The impacts of the climate change on the water resources are assessed by comparing the results of the hydrologic model run under present and warm up conditions. The daily values of the temperature, precipitation, and the potential evapotranspiration estimated by the data provided by the Dr. Kimura's Climate Subgroup for the periods of 1993 to 2004 and 2070 to 2080 are used to reflect the water circulation under present and global warming conditions. The mean values of the climate variables are given in Figure 6.1. The spatial averages of these parameters are given in Table 6.1. The grid size of the climate input given to the hydrologic model is about 8 km, whereas the model cell dimension is 1 km.

Table 6.1. The Spatial Average Values of the Annual Temperature, Precipitation and Potential Evapotranspiration in Seyhan River Basin

	Present (1993-2004)			MRI (2070-2080)			CCSR (2070-2080)		
	Mean	Min	Max	Mean	Min	Max	Mean	Min	Max
Temperature (°C)	12.3	6.2	20.3	14.3	8.3	21.8	15.3	9.3	22.7
Precipitation (mm)	681.3	451.6	1313.5	514.9	324.9	1004.9	455.9	303.7	968.9
Pot.Evapotranspiration (mm)	433.1	328.4	669.9	469.8	350.5	697.0	495.8	367.9	750.1

The results of the MIKE SHE simulations for present and warm up conditions are summarized in Table 6.2. The figures in Table 6.2 reflect the percent decrease of the water budget elements with respect to present conditions. The CCSR climate data results more decrease than the MRI data. The decrease in the actual evapotranspiration is limited because of the decrease in the precipitation. The decrease in the precipitation in warm up period is 29.4 % and 34.7%, which causes 37.5% and 46.4% decrease in the river flow. The groundwater recharge in whole Seyhan Basin decreases 24.7% - 27.4%. The majority of the springs in the basin become dry due to decline of the groundwater level below the spring level.

The temporal change of the river flow is depicted on Figure 6.2, at 18-18 gauging site on Seyhan River. The peak discharge decreases in both MRI and CCSR projections. The month for the peak flow is same in present and warm up period, but the volume decreases radically.

Table 6.2. The Percent Decrease of the Water Budget Elements in Warm up Period with Respect to Present Conditions

	MRI	CCSR
Precipitation	29.4	34.7
Actual Evapotranspiration	16.9	16.9
River Flow	37.5	46.4
Discharge to the Mediterranean Sea	50.0	54.2
Recharge	24.7	27.4
Spring Discharge	50.0	50.0

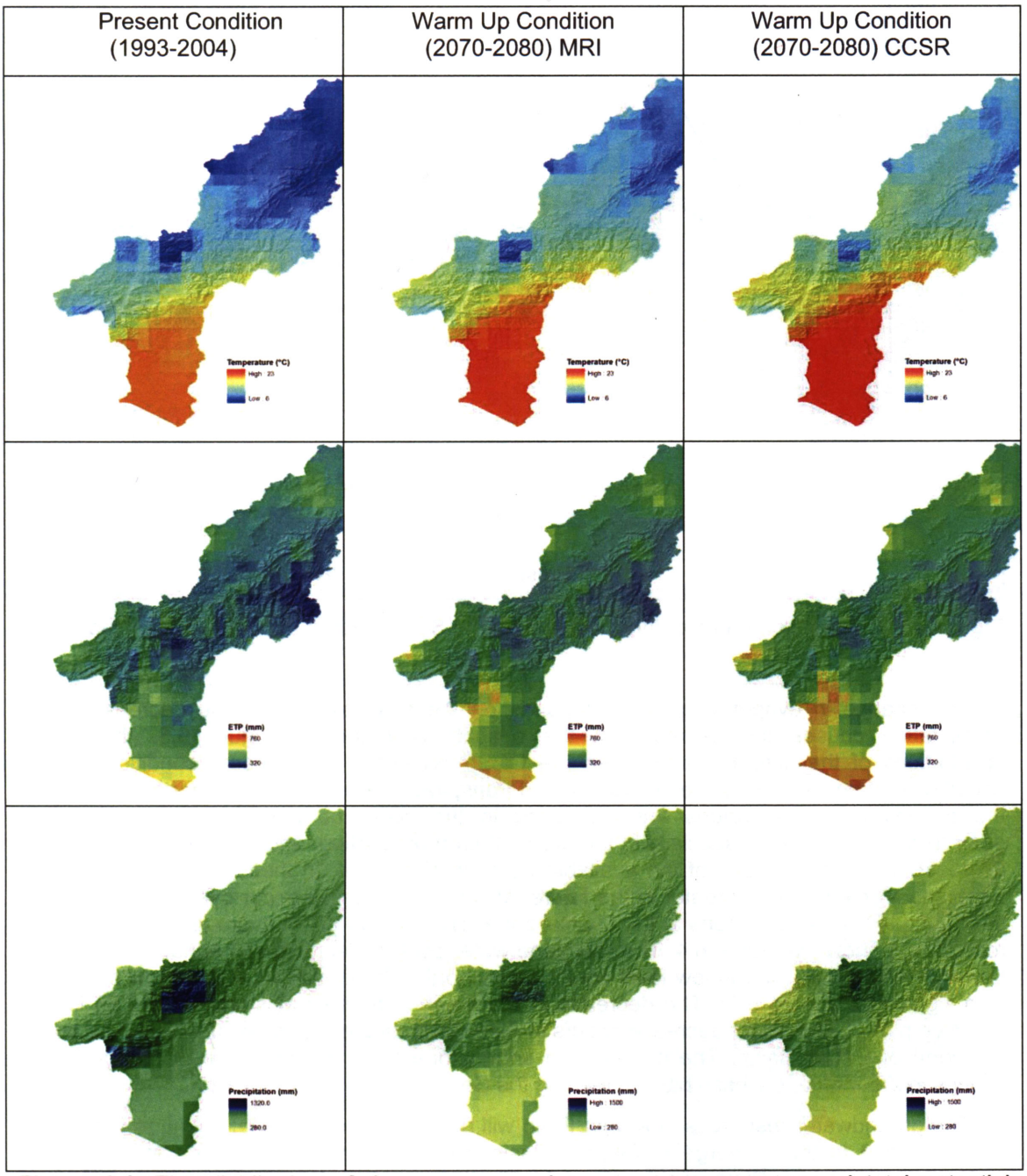

Figure 6.1. The distribution of the mean annual temperature, mean annual total potential evapotranspiration and mean annual total precipitation for present (1993-2004) and for warm up (2070-2080) periods estimated by MRI and CCSR data

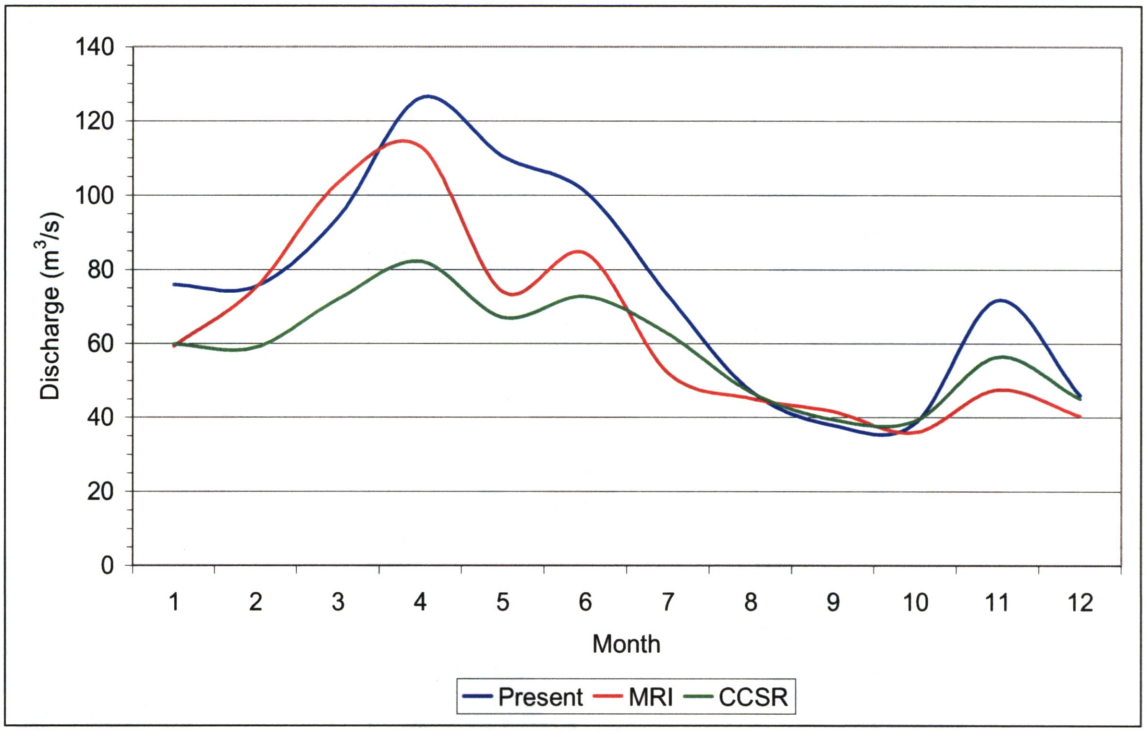

Figure 6.2. Change in mean monthly discharge of the Seyhan River at 18-18 gauging station

The change in evapotranspiration depends on the available water. The decrease in the precipitation causes the decrease in the evapotranspiration. In Figure 6.3, the spatial distributions of the differences between the CCSR projection and present conditions of the actual evapotranspiration, soil evaporation, and transpiration are given. In the north of the basin, the evapotranspiration values are increasing in the warm up period, whereas they are decreasing in the south, especially in the areas of crop production, and natural vegetation. The decrease is due to the lack of the available water to evaporate. In these zones, the irrigation water requirement will be greater in the future. Maximum increases occur over the branches of the Seyhan River, and lagoons at the coastal zone. The change of the average water content in root zone is shown in Figure 6.4. The root zone water content decreases in agricultural areas in Lower Seyhan Plain, and in low level zones at the north. The decrease of the snow storage is also significant (Figure 6.5). The decrease in the mean annual snow storage is 14.56 km^3 in warm up period. The major decrease occurs in Aladağlar, southeast slopes of the Erciyes and in the north of Göksu Basin. The decrease in snow storage will influence the discharge of the springs in Zamantı and Göksu basins, feeding the Seyhan River.

The groundwater resources in Adana Plain will be influenced by climate change drastically. The decrease in the recharge in Seyhan Basin will cause the decrease in the subsurface recharge to the Adana Plain from north, and infiltration over the plain. Additional loss will occur due to increase in the abstraction in warm up period to comply the irrigation water requirement. The water budget for the groundwater system in Adana Plain is given in Figure 6.6, whereas the change in the groundwater storage is given in Figure 6.7.

The groundwater resources in the Adana Plain are highly susceptible to the climate change. The most important impacts are the decrease in the recharge in higher elevations, and increase in the abstraction due to the limitations in surface water resources. The decline in the head will also cause saline water intrusion. The simulations indicate that the intrusion length is controlled by the groundwater level in the plain. In case of % 50 increase of the groundwater abstraction in warm up conditions, the length of the sea water intrusion will reach 10 km inland (Figure 6.8) at the end of 2080.

The decline in the storage will be accompanied with the quality degradation in the

groundwater resources. In the coastal zone of the Adana Plain, the groundwater salinity will reach 25% of sea water composition.

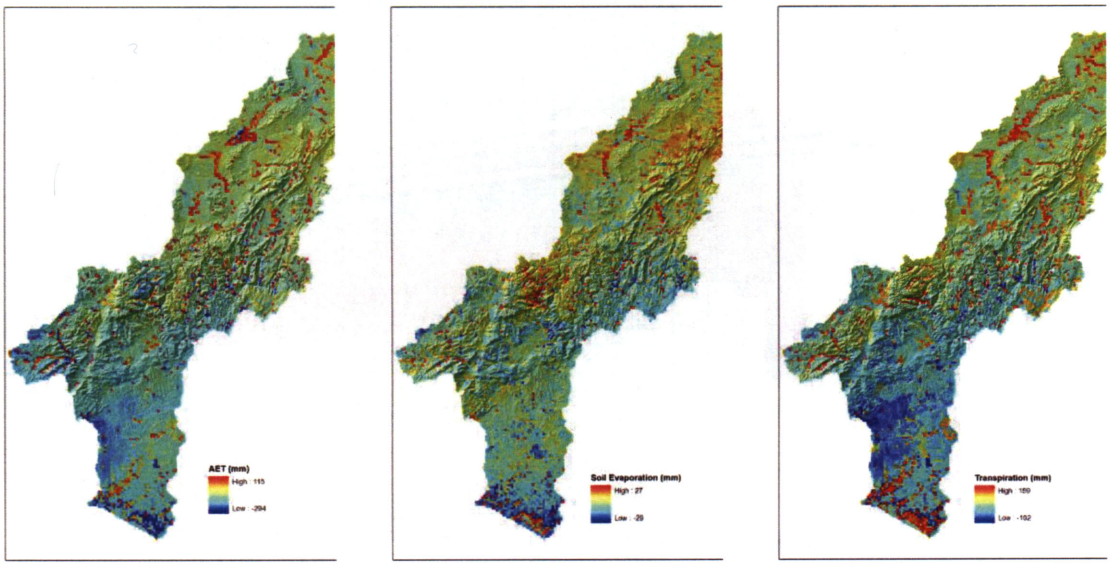

Figure 6.3. Change of the actual evapotranspiration, soil evaporation, and transpiration, positive values indicate increase, negative values indicate decrease with respect to present conditions.

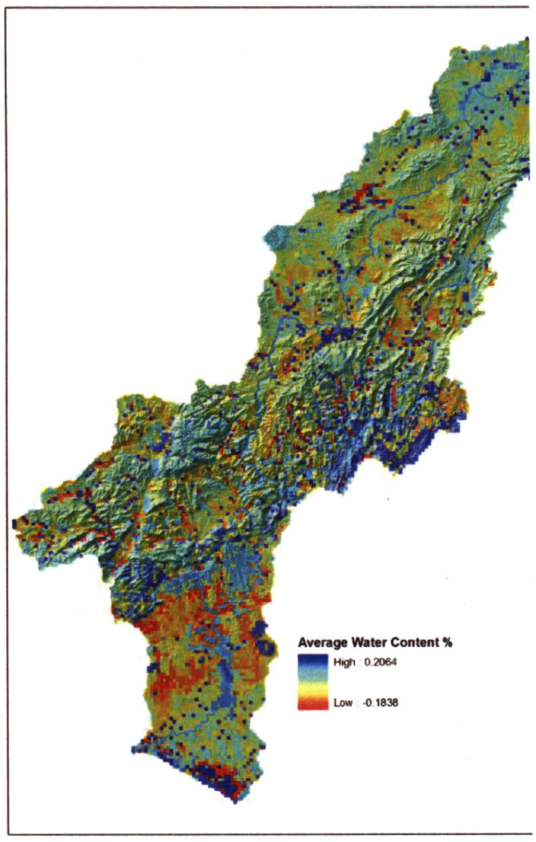

Figure 6.4. The change of the Average Water Content in root zone in warm up conditions

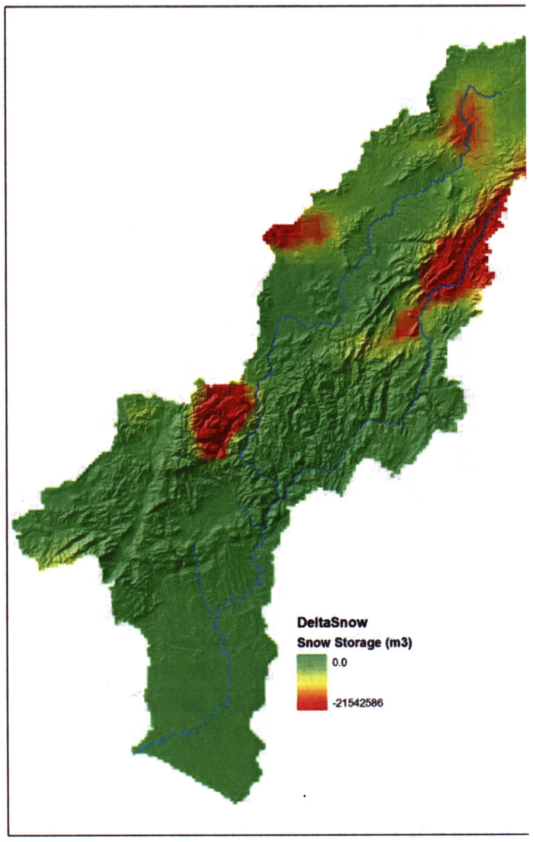

Figure 6.5. The decrease of the snow storage in warm up conditions

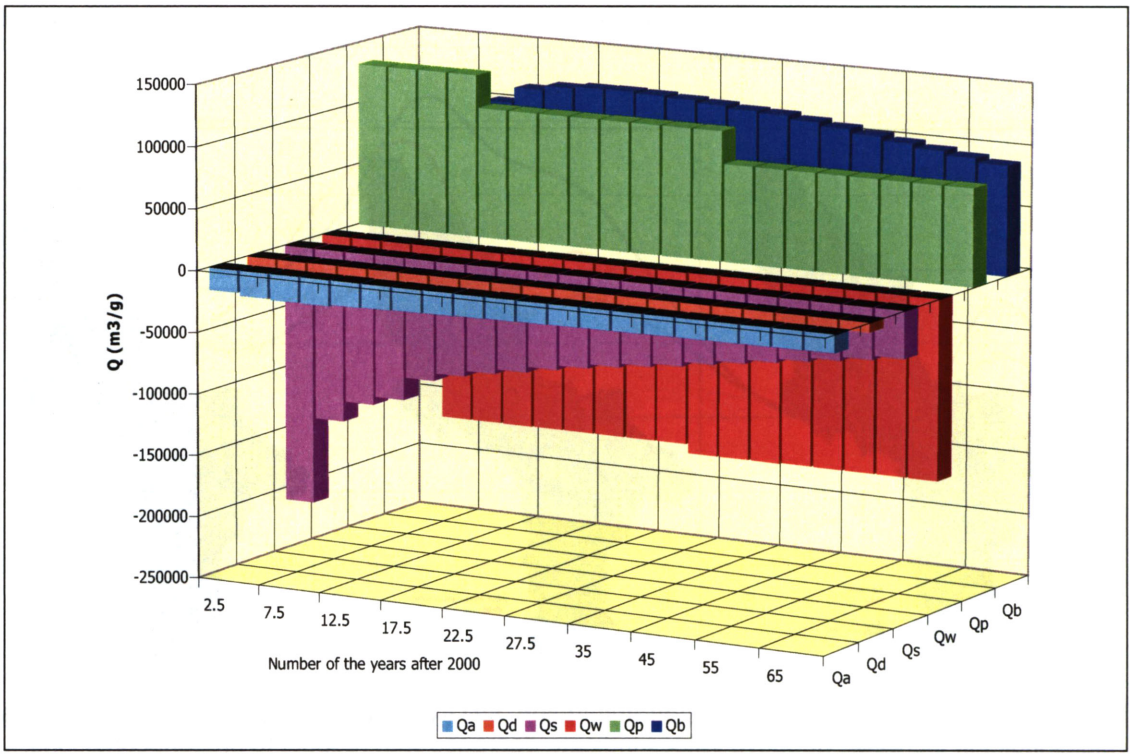

Figure 6.6. Components of the water budget calculated by the model (Qb: inflow from the northern border, Qp: recharge from precipitation, Qw: abstraction by wells, Qs: outflow to the sea, Qd: drainage by drainage canal, Qa:

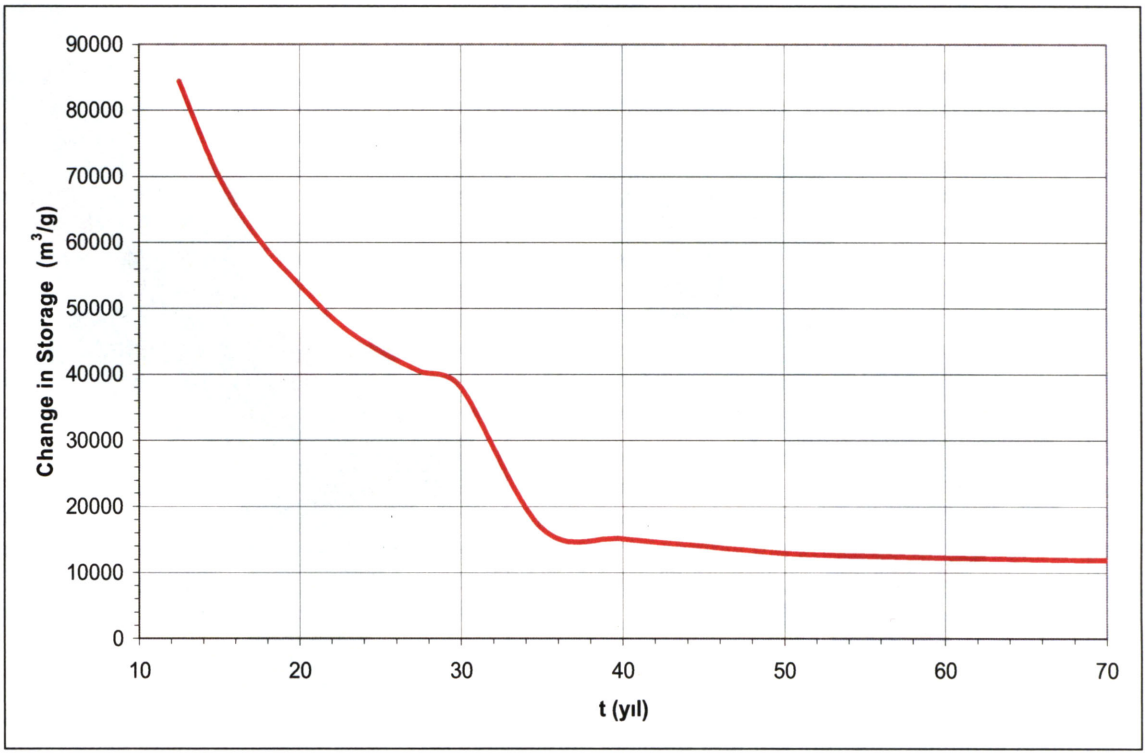

Figure 6.7. The impact of the climate change on the ground water storage in Adana Plain

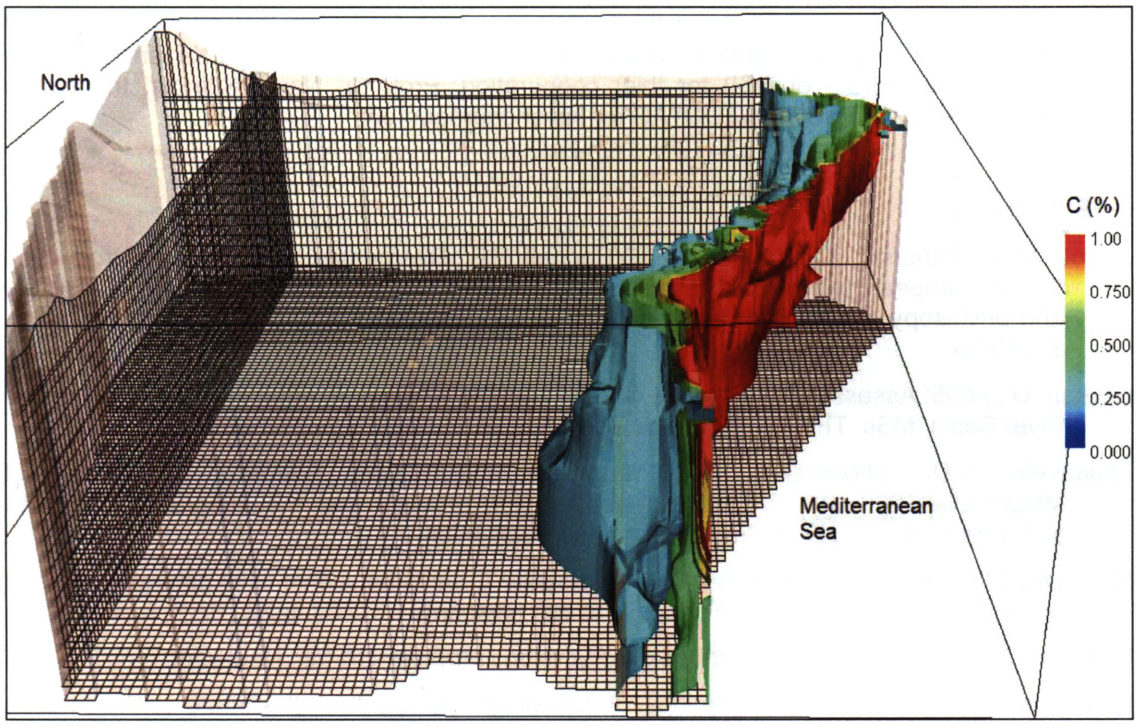

Figure 6.8. The sea water intrusion in the year of 2080

7. Conclusions

The climate change impacts on the water resources of the Seyhan River Basin are evaluated in basin scale by physically based hydrologic models. All the elements of the hydrologic cycle are considered with in a comprehensive hydrology model. The temporal and spatial distribution of the changes in the water resources potential are calculated, by using the climate variable estimations, downscaled from two different GCMs.

It is necessary to emphasize that the values given in this report are based on many assumptions, including the fundamental scenarios of the GCM estimations. The conceptualization and parameterization of the hydrologic model have been based on very limited data and field observations. The temporal and spatial representativity of the available data are very low. Many data and parameter required by the model were derived from secondary sources. Thus, the actual figures may deviate from the values given here. However, the tendency of the change will be similar, if the scenarios of the GCM would occur.

The management of the water resources in the warm up conditions will require more precise and extensive data. The continuous observations of the hydrologic cycle are essential for sustainable utilization of the water resources.

The climate change will result the reduction of the input to the basin, and all types of the water resources will be influenced by these reduction. The surface water resources, the snow storage, and groundwater resources will decrease drastically. The water requirement for the agricultural production and natural vegetation will increase. Therefore efficient utilization of the water resources in all sectors, water saving, control of the water usage, extension of the observation network, enlargement of the artificial storage potential in the basin are high priority management issues to be prepared for warm up conditions.

8. Acknowledgement

This research was partially supportaed by TÜBİTAK-TOGTAG. Within the framework of the project number TOGTAG-JPN09 " Assessment of Vulnerability of Water Resources of the Seyhan River Basin Against Climate Change" The researchers involved in this study are thankful to Prof. Dr. Rıza Kanber (Coordinator of the Turkish Team of the ICCAP), Prof. Dr. T.

Watanabe (Leader of the ICCAP) for theri efforts to resolve all technical and administrative problems; Prof. Dr. Veysel Eroğlu (General Director of the DSI) and Mr. Sırrı Kazancı (Director of the Adana Directorate of DSI) for thier cooperation. Prof. Dr. Neşet Kılınçer, the former Executive Secretary of TUBİTAK-TOGTAG for his encouragement.

9. References

Abbott, M.B., Bathurst, J.C., Cunge, J.A., O'Connell, P.E., Rasmussen, J., 1986: An introduction to the European hydrological system-Systeme hydrologique Europeen, SHE 1. History and phylosopy of a physically based distributed modeling system. Journal of Hydrology, 87, 45-59.

Gürkan, D., 2005: Assessment of climate change impacts on surface water resources in Seyhan River Basin, MSc. Thesis, Hacettepe University (in Turkish, unpublished)

Langavein, C.D., Shoemaker, W.B., and Guo, W., 2003: SEAWAT: A version of MODFLOW-2000 with the variable-density flow process and the integrated MT3DMS transport process. USGS Water Resources Publication.

McDonald M.G. and Harbough, A.W., 1988: A modular three dimensional finite difference ground water flow model, USGS Techniques in Water Resource Investigations, Book 6, 586.

Maidment, D.R. (Editor), 1993, Handbook of Hydrology,McGraw-Hill Inc.,New York.

Rodriguez-Iturbe, I, 2000: Ecohydrology: A hydrologic perspective of climate-soil-vegetation dynamics. Water Resources Research, 30 (1), 3-9.

Van Genuchten, M.Th., 1980: A closed-form equation for predicting the hydraulic conductivity of unsaturated soils. Soil Sci. Soc. Am. J. 44, 892-898

Webb, W.B., and Walling, D.E. 1996: Water qualiy II. Chemical characteristics. In River Flows and Channel Forms (ed. G Petts and P. Calow) Chapter 6, pp 102-129, Blackwell Sci. Cambridge, Mass.

Yalcınkaya S.O., 2005: The impacts of the climate change in Adana plain on the groundwater level and sea water intrusion, MSc. Thesis, Hacettepe University (in Turkish, unpublished)